Available online at www.sciencedirect.com
SCIENCE DIRECT
Applied Surface Science 208–209 (2003) 194–198
applied surface science
www.elsevier.com/locate/apsusc

Fatigue behaviour of laser machined 2024 T3 aeronautic aluminium alloy

F.J. Carpio[a], D. Araújo[a,*], F.J. Pacheco[a], D. Méndez[a], A.J. García[a], M.P. Villar[a], R. García[a], D. Jiménez[b], L. Rubio[b]

[a]Departamento de Ciencia de los Materiales e Ingeniería Metalúrgica y Química Inorgánica, Universidad de Cádiz, 11510 Puerto Real, Cadiz, Spain
[b]EADS-CASA, Avda Marconi 33, 11011 Cadiz, Spain

Abstract

High power laser applications as welding, machining and marking are widely used in several industrial sectors to take advantage of their high processing velocity, clean processing conditions, and a high versatility. However, the heat affected zone (HAZ) is expected to change the mechanical behaviour of laser processed structural elements. For aeronautic applications, this feature is of first importance because those elements suffer cyclic stress under service conditions. Indeed, the most severe requirements for further industrial implantation are the fatigue specifications. In this communication, fatigue behaviour of laser machined 2024 aluminium alloy is studied to evaluate a possible certification of laser-based machining in the aeronautic industry. For this reason, 1.6 mm thick samples laser machined were carried out using a CO_2 laser. The experimental fatigue curves are shown to lie very close to aeronautic requirement despite theoretical fatigue behaviour of the material is significantly more resistant. This is attributed to surface roughness induced by a surface melting zone shown that diminish the fatigue resistance. Fatigue behaviour and surface roughness should be improved using higher power and/or high absorption wavelength as that of YAG laser ($\lambda = 1.06$ μm).

PACS: 42.62.C; 62.20.M; 81.40.N

Keywords: Laser machining; Aluminium 2024 T3; Fatigue

1. Introduction

Nowadays, laser technologies, as cutting and machining are able to take place for different industrial applications. Among them, it is a suitable method for the aeronautic industry sector due to processing velocity of individual operations, cleanness in terms of acoustic and dust considerations and versatility [1] making possible its robotisation or individual sheet machining.

Among the aeronautic materials, Al alloys are one of the most promising for laser machining implantation, despite its absorption is very low (∼1% room temperature, 7.7% melt) [2]. Al–Zn–Mg alloys are restricted also for laser machining due to their environmental sensitive fracture in service [3]. This can be improved by the addition of Cu (7475 alloy [4] or 2xxx series) but the latter is also known to degrade the laser cutting quality [5]. Even though laser processing has been shown to improve the fatigue resistance for the

* Corresponding author. Tel.: +34-956-016351; fax: +34-956-016288.
E-mail address: daniel.araujo@uca.es (D. Araújo).

0169-4332/02/$ – see front matter
doi:10.1016/S0169-4332(02)01369-7

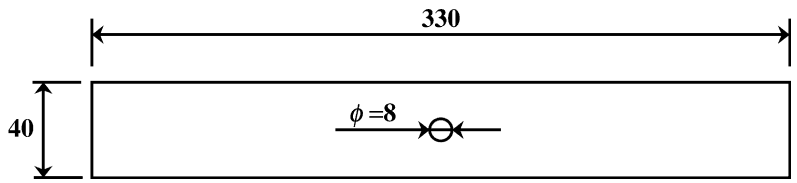

Fig. 1. Schematic description of the sample geometry. It consists in a 2024 T3 aluminium sheet of 1.6 mm thick, 330 mm length and 40 mm large. The laser machining performs a central hole of 8 mm diameter by orbital drilling to obtain a concentrator factor $K_t = 2.5$.

case of aluminium superficial treatment (laser shock peening (LSP)), as a result of the increased dislocation density, decrease of surface roughness and resulting compressive residual stress [6–8]. For the case of machining, the material reaches high temperatures that should modify this behaviour in terms of thermal conductivity and absorption coefficient [9].

Aluminium 2024 T3 is a typical aeronautic alloy used for structural elements as fuselage or lower wing surfaces due to its extremely good damage tolerance and high resistance to fatigue crack propagation in T3 aged condition [10]. However, during the laser processing, materials microstructure around the processed zone is damaged, promoting the cracks formation [5]. Therefore, an evaluation of its implications is necessary. The most critical requirement is a possible reduction of the fatigue resistance. In this study, fatigue behaviour of mechanical and laser machined samples are experimentally compared according to Airbus Industrie Test Method (AITM) standard [11], using test samples T-type (geometry of test samples) $K_t = 2.5$ (stress concentration factor).

Fatigue crack results are statistically treated based on American Society for Testing and Materials (ASTM) E739 standard [12] and analysed according to aeronautic standards AITM [11] and Airbus Industrie Material Specification (AIMS) [13].

First the fatigue experimental design for laser and traditional machined samples is presented; second, experimental results and *S–N* curves are presented for longitudinal and transversal laminated sheets, and finally these curves are compared to standard ones.

2. Experimental

Tested material is Al 2024 T3. The material main components are, in addition to aluminium, copper (4.4% content) and magnesium (1.5% content). Fatigue testing were made on three series of samples. The first series, series A, 15 samples was mechanically machined (tool material HSS with lubricant assistance, machining velocity: 600 rpm) having superficial aluminium cladding called AlClad. The second and the third series, series B and C, were CO_2 laser machined and in both cases, 20 samples were tested. Laminating direction was the difference, being either transversal or longitudinal. AITM standard [11] gives the basis for samples dimensions, $330\,\text{mm} \times 40\,\text{mm} \times 1.6\,\text{mm}$ with a 8 mm diameter hole as shown in Fig. 1. Tests were carried out on a Suzpecar MUF-20 fatigue tester coupled to Suzpecar software (Version F-105) for data acquisition.

Fatigue tests were made at four stress levels for laser machined samples, series B and C, from 193 to 101 MPa, with five samples for each stress level, resulting an answer level of 80%. The stress ratio was $R = 0.1$ with constant stress [13]. The used frequency was 10 Hz (below 170 Hz, maximum required frequency). In agreement with ASTM E739 [12], tests have a 60% replication, being "design allowable data" for the first experimental series (mechanically machined samples). In second and third experimental series (laser machined samples), tests have a 95% replication, being "reliability data".

The reference values are obtained from two different sources: standard aeronautic curves and ASM Metal Handbook [14] using master diagram curves to adequate the *S–N* curve (stress–number of cycles to failure) for the experimental cycles required ($R = 0.1$, $K_t = 2.5$).

3. Results

Fig. 2 compares the experimental fatigue life data at four different levels. To each level corresponds four

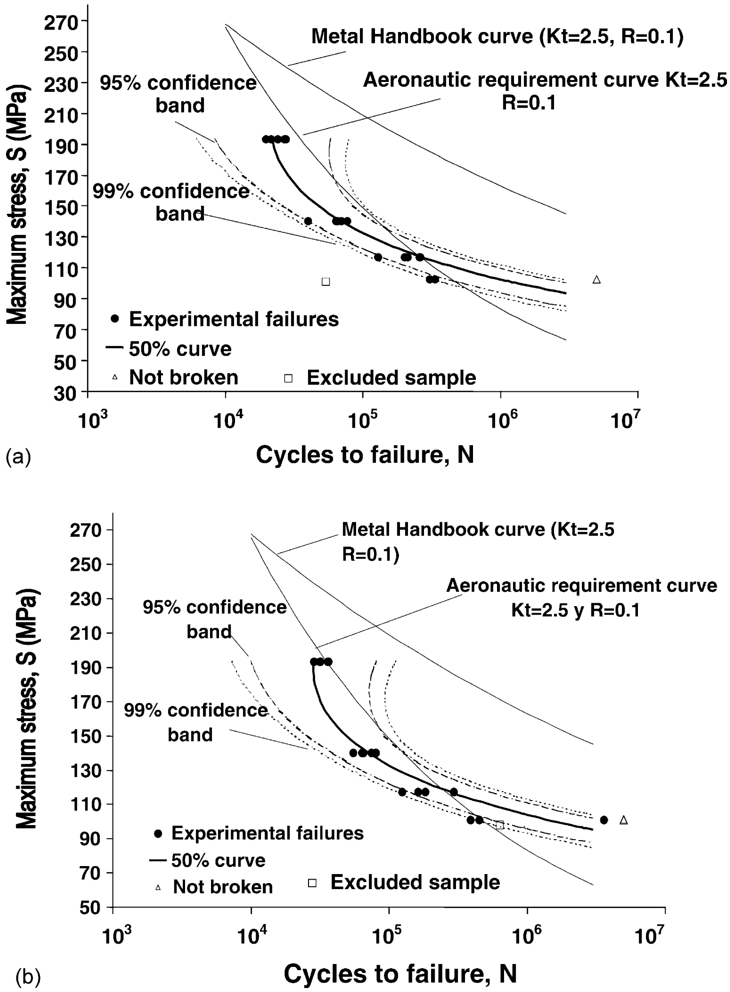

Fig. 2. Experimental fatigue life data (black points) versus maximum stress compared with reference curve for series B and C. Statistical parabolic fits (following ASTM E 379 standard) with their respective confidence curves at 99 and 95% are also displayed (dashed lines). Note that the fatigue experimental conditions are performed at $R = S_{max}/S_{min} = 0.1$ and $K_t = 2.5$; correspond to test sample (a) with a transversal laminate, and (b) with a longitudinal laminate.

tests to fracture. Therefore, the percent replication amounts to 95% and is considered as reliability data [12]. Computed value is defined as follows:

$$\frac{\sum_{i=1}^{L} m_i(\hat{Y}_i - \bar{Y}_i)^2/(L-2)}{\sum_{i=1}^{L}\sum_{j=1}^{m_i}(\hat{Y}_{ij} - \bar{Y}_i)^2/(k-L)} \quad (1)$$

where $Y_i = \log \varepsilon_i$ being ε_i deformation, $\hat{Y}_i$ the estimated value, $\bar{Y}_i$ the average value, K the number of tested samples, L the stress levels, and m_i is the replication at Y_i.

When the computed value exceeds the $F_p = 3.6$ (value from Table 2 in ASTM E379 [12]), non-linear model is required to fit the experimental values:

$$\mu_{X/Y} = A + BY + CY^2 \quad (2)$$

The fitting parameters are for the transversal and longitudinal laminate $A = 157.6$, $B = -136.6$, $C = 30.5$, and $A = 138.1$, $B = -118.0$, $C = 26.1$, respectively. The data dispersion at low stress levels seems to be in part due to the accuracy of the testing

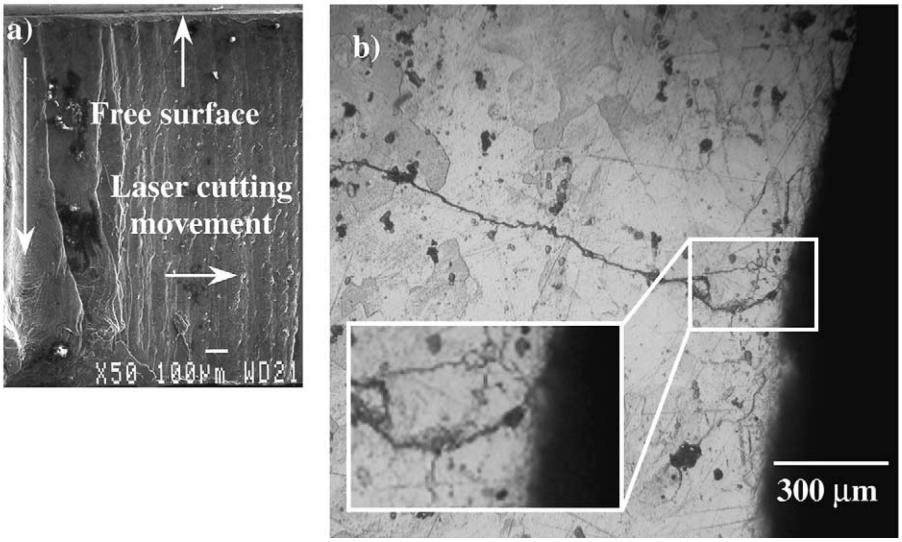

Fig. 3. (a) Transverse view scanning electron microscopy (SEM), and (b) planar view optical microscopy micrographs showing surface roughness and grain size of a laser processed sample. The second micrograph evidence a fatigue crack initiation at a stress concentration defect of laser machined surface.

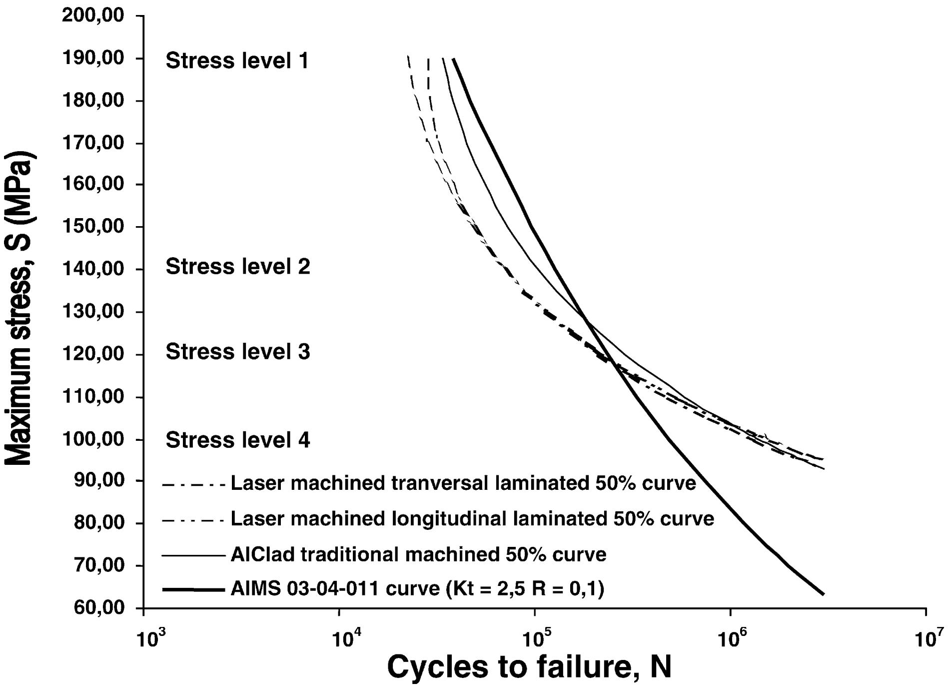

Fig. 4. Comparison of the *S–N* curve for the laser machined longitudinal laminate sheets (Al 2024 T3, series C), transversal laminate ones (Al 2024 T3, series B) and mechanically machined ones (AlClad 2024, series A).

machine and to statistical crack initiation at stress concentration of the roughened surface. For both sets of samples the aeronautic requirements are shown to surround the experimental data. However, ASM Metal Handbook estimated values lies much above the experimental ones. To confirm roughness induces crack initiation, scanning electron microscopy (SEM) and optical microscopy investigations after polishing and Keller wet etching, are presented in Fig. 3. The micrographs are taken just at the crack initiation state. Transgranular propagation is observed in Fig. 3b in addition to initiation at a microconcentrator defect induced by the surface roughness. The melted material seems to be responsible for such roughness.

The increase of the absorption coefficient by a factor 7 when Al melts leads the material to cross a transient liquid phase step in spite of a direct sublimation. This should probably be improved using a YAG laser source ($\lambda = 1.06$ μm) as absorption coefficient increases significantly for the solid state values. Fig. 3a shows also fringes perpendicular to the laser displacement even continuous wave (CW) mode is used here. Their origin is not yet completely understood. The fringes are not rigorously parallel and their separation can not correspond to laser motorization related artefacts.

Fig. 4 compares the 50% laser machined curves (series B and C) to mechanically machined (series A) and reference curves. The mechanical drills were performed at acceptable standard aeronautic quality. However, roughness at shrivelled seems to be responsible for the low *S–N* curve respect to standard ones. Indeed, laser results are comparable to mechanically processed ones.

4. Conclusions

Fatigue behaviour study of Al 2024 T3 laser machined sheets was performed in order to estimate a possible certification of the procedure. Laser based and mechanically machined samples present higher resistance fatigue than expected. As a result, aeronautic requirements curves are very close to experimental values. Both, longitudinal and transversal laminate samples, have a similar fatigue resistance. However, intrinsic material fatigue resistance predictions for identical cycling *conditions* are still above the laser machined experimental data. This is attributed to surface roughness of the heat affected zone (HAZ) surface, promoting crack initiation. The mechanisms responsible for this surface state has been presented recently [10].

In addition to AlCu phase diagram considerations, CO_2 laser source wavelength ($\lambda = 1.06$ μm) irradiation suffers a very low light absorption coefficient. This problem should be solved using a YAG laser source ($\lambda = 1.06$ μm).

References

[1] N. Tabata, Y. Dhigenori, M. Hishii, J. Mater. Process. Technol. 62 (1996) 309.
[2] H. Brücher, J.H. Schäfer, J. Uhlenbasch, J. Appl. Phys. 66 (1989) 1321.
[3] M.T. Jahn, J. Luo, J. Mater. Sci. 23 (1988) 4115.
[4] B.B. Verma, J.D. Atkinson, M. Kumar, Bull. Mater. Sci. 24 (2) (2001) 231.
[5] D. Araújo, F.J. Carpio, D. Mendez, A.J. García, M.P. Villar, R. García, D. Jiménez, L. Rubio, Appl. Surf. Sci., in press.
[6] Z. Hong, Y. Chengye, Mater. Sci. Eng. A 257 (1998) 322.
[7] K.K. Zhang, X.R. Zhang, X.D. Wang, S.Y. Zhang, L.Y. Gao, J.Z. Zhon, J.C. Yang, L. Cai, Mater. Sci. Eng. A 297 (2001) 138.
[8] J.H. Yang, Y.C. Her, M. Han, S. Klein, H. Naff, J.H. Schäfer, Mater. Sci. Eng. A 298 (2001) 296.
[9] J. Uhlenbasch, V. Bielesch, S. Klein, H. Naff, J.H. Schäfer, Appl. Surf. Sci. 106 (1996) 228.
[10] J. Zehnder, in: D.G. Altenpohl (Ed.), Aluminium: Technology, Application and Environment: A Profile of a Modern Metal, TMS Warrendale, Pennsylvania, p. 319.
[11] AITM 1-0011, Constant Amplitude Fatigue Testing of Metallic Materials.
[12] ASTM E739, Standard Practice for Statistical Analysis of Linear or Linearized Stress-Life (*S–N*) and Strain-Life (ε–*N*) Fatigue Data.
[13] AIMS 03-04-011, Aluminium Alloy (2024): Solution Treated and Naturally Aged (T3), Clad Sheet 0.2 mm, $a = 6.0$ mm, Special Surface Quality, Material Specification.
[14] Fatigue and fracture, ASM Metal Handbook, vol. 19, AMS International, USA, 1996.